Journal of Photonics for Energy

SPIEDigitalLibrary.org/jpe

Thin-film transistor as a probe to study carrier transport in amorphous organic semiconductors

Shu K. So
Wing H. Choi
Chi H. Cheung

SPIE

Thin-film transistor as a probe to study carrier transport in amorphous organic semiconductors

Shu K. So, Wing H. Choi, and Chi H. Cheung
Hong Kong Baptist University, Department of Physics and Center for Advanced Luminescence Materials, Kowloon Tong, Hong Kong, China
skso@hubu.edu.hk

Abstract. We describe how to use the thin-film transistor (TFT) technique to quantify carrier transport of amorphous organic semiconductors relevant to organic electronic devices. We have chosen several amorphous materials, including arylamine compounds, 4,4′-N,N′-dicarbazole-biphenyl (CBP), and a phosphorescent dye molecule [$Ir(ppy)_3$] for investigations. Generally, the field effect (FE) mobility was found to be about one order of magnitude smaller than that obtained from an independent time-of-flight (TOF) technique. For N′-diphenyl-N,N′-bis(3-methylphenyl)-(1,1′-biphenyl)-4,4′-diamine (TPD) and N,N′-Bis(3-methylphenyl)-N,N′-bis(phenyl)-9,9-spirobifluorene (spiro-TPD), the FE mobilities were found to be 1.7×10^{-5} and 1.3×10^{-5} cm^2/Vs, respectively. Temperature-dependent measurements were carried out to study the FE mobility. It was found that the energetic disorder increased in the neighborhood of a gate dielectric layer. This factor is one of the origins causing the discrepancy between TFT and TOF mobilities. We also examined how the hole transport of CBP is affected by $Ir(ppy)_3$ when it is doped into CBP. © *2011 Society of Photo-Optical Instrumentation Engineers (SPIE)*. [DOI: 10.1117/1.3534200]

Keywords: thin-film transistors; hole transports, 4,4′-N,N′-dicarbazole-biphenyl (CBP); tris(2-phenylpyridine) iridum [$Ir(ppy)_3$]; organic light-emitting diodes (OLEDs).

Paper 10111SSPR received Jul. 14, 2010; revised manuscript received Dec. 7, 2010; accepted for publication Dec. 14, 2010; published online Feb. 3, 2011.

1 Introduction

Organic electronics has grown tremendously over the past 20 years due to its broad applications in photonic devices. Examples are organic light-emitting diodes (OLEDs), organic thin-film transistors (OTFTs), and organic photovoltaic cells.[1–3] Among these devices, phosphorescent organic light-emitting diodes (PHOLEDs) have captured considerable attention due to their extraordinarily high power efficiencies. OLEDs exceeding 100 lm/W have been reported and are seriously considered to be the next-generation ultrathin solid state lighting devices.[4] Irrespective of the precise nature of these devices, charge-carrier transport remains one of the most critical issues in understanding the device operations. In fact, the ability of quantifying the carrier transport of an organic semiconductor is essential for device development and optimization.

There are abundant techniques for studying carrier transport.[5] In this contribution, we demonstrate how to employ thin-film transistor (TFT) technique to study the hole transporting properties of amorphous organic semiconductors. Generally, TFT technique is not viewed as the most appropriate tool to study intrinsic carrier transport of an organic semiconductor due to the presence of a gate dielectric layer. The gate dielectric may conceivably affect charge transport in two ways. (*i*) The orientations of the organic molecules could be different in the neighborhood of a gate dielectric layer. Thus, charge transport could be very different from the case in which the gate dielectric layer is absent. (*ii*) The gate dielectric may modify the energy landscape of charges hopping in its neighborhood. In the case of an amorphous organic semiconductor,

1947-7988/2011/$25.00 © 2011 SPIE

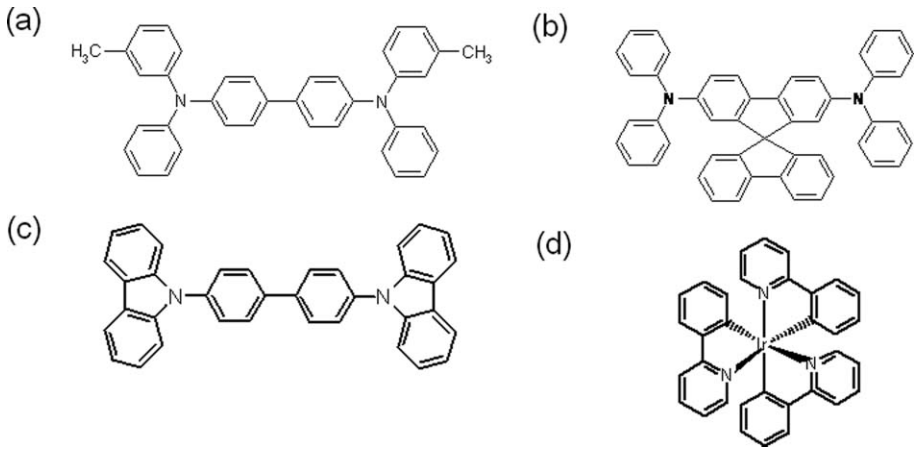

Fig. 1 Chemical structures of (a) TPD, (b) spiro-TPD, (c) CBP, and (d) $Ir(ppy)_3$.

the first limitation is removed because the orientations of the molecules are random. Yet, the second limitation remains. In this contribution, we show how to delineate factor (*ii*) from TFT data using data obtained independently from a time-of-flight (TOF) technique. We examine the feasibility of the TFT technique to study the hole transport properties of two arylamine compounds, N′-diphenyl-N,N′-bis(3-methylphenyl)-(1,1′-biphenyl)-4,4′-diamine (TPD) and N,N′-Bis(3-methylphenyl)-N,N′-bis(phenyl)-9,9-spirobifluorene (spiro-TPD).[6,7] Extensions of the TFT technique to study the charge conducting properties of tris(2-phenylpyridine) iridum [$Ir(ppy)_3$] and 4,4′-N,N′-dicarbazole-biphenyl (CBP), will be presented. The chemical structures of all molecules studied are shown in Fig. 1. From x-ray-diffraction and ellipsometery experiments, neat films of TPD, spiro-TPD, and CBP were known to form smooth amorphous films.[8,9] The structure of $Ir(ppy)_3$ film is not known, but it has a molecular structure similar to another metal chelate tris(hydroxyquinoline) aluminum (Alq_3), which is also known to form an amorphous film.[8,9] In phosphorescent OLEDs, CBP is generally used as a host material for $Ir(ppy)_3$.[10] When $Ir(ppy)_3$ is doped into CBP, CBP molecules facilitate energy transfer to $Ir(ppy)_3$. But a sound understanding of the carrier transport property in the doped system is still unknown. Thus, we have also taken the transport measurements on $Ir(ppy)_3$ doped into CBP. Figure 2 shows the work functions and energy levels of all materials used in the experiments. Typically, we use gold (Au) as the source and drain electrodes in a *p*-type OTFT. The work function of Au is ∼5.1 eV. In a $Ir(ppy)_3$-based OTFT, hole injection is effective as the highest occupied molecular orbital (HOMO) of $Ir(ppy)_3$ is only about 5.2 eV.[10] But, in the case of CBP, it has a relatively large HOMO value of ∼5.7 eV.[11] To facilitate hole injection, a thin layer of molybdenum oxide (MoO_x), which has a relatively high work function of between 5.6 and 6.7 eV, was inserted between the organic layer and gold (source/drain) electrode.[12,13]

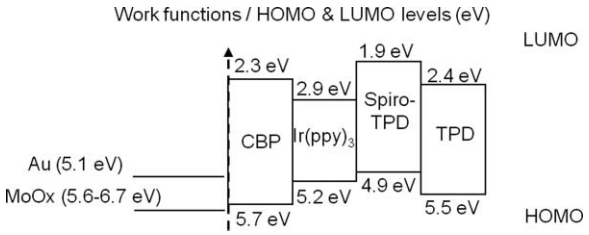

Fig. 2 Energy levels of corresponding materials.

2 Experimental Details

CBP was purchased from E-ray while TPD, spiro-TPD, and $Ir(ppy)_3$ were purchased from Luminescence Technology Corporation. A heavily doped silicon (p-Si) wafer, etched with a 300 nm thin layer of SiO_2, was used as the substrate. The dielectric capacitance per unit area C_i of the Si wafer substrate is 11 $nFcm^{-2}$ as measured by an impedance analyzer. Before the deposition of organic film, the substrate was cleaned by ethanol and acetone in an ultrasonic bath, followed by UV-ozone treatment.[14] An organic layer was deposited on the pretreated substrate by thermal evaporation at high vacuum. The coating rate and thickness of the organic film were 0.5 Å/s and 100 nm, respectively. The thickness was monitored by a quartz-crystal sensor. In the case of $Ir(ppy)_3$-doped CBP films, the coating rates for both organics were equal to 1 Å/s. The concentrations of $Ir(ppy)_3$ in CBP were 0, 0.5, 10, 20, 50, and 100%. Subsequently, 20 nm of MoO_x capped with a 100 nm of gold (Au) were thermally deposited via a shadow mask to define the source and drain electrodes.[15,16] After the fabrication, the sample was loaded into a vacuum cryostat. The sample temperature was regulated between 237 and 377 K for the TFT measurement. From the TFT data, field-effect (FE) mobilities from both the linear and saturation regions were evaluated using the standard equations,[17]

$$\text{Linear region:} \quad I_{DS,Lin} = (W/L)\mu_{FE,Lin}C_i\left[(V_G - V_T)V_{DS} - (V_{DS}^2/2)\right]. \tag{1}$$

$$\text{Saturation region:} \quad I_{DS,Sat} = (W/2L)\mu_{FE,Sat}C_i(V_G - V_T)^2. \tag{2}$$

In Eqs. (1) and (2), W and L are, respectively, the channel width and length of the OTFT; C_i is the capacitance of the gate dielectric per unit area; V_{DS} and V_G are, respectively, the voltage applied to the drain and gate electrode; V_T is the threshold voltage and μ_{FE} is the FE mobility. Under the linear region, the FE mobility $\mu_{FE,Lin}$ could be extracted from the slope of I_{DS} versus V_G plot. Similarly, at the saturation region, the FE mobility $\mu_{FE,Sat}$ could be extracted from the slope of $(I_{DS})^{1/2}$ versus V_G plot.

3 Results and Discussion

3.1 *Transport Measurement of Arylamine Compounds*

Figure 3 shows the output characteristics (I_{DS} versus V_{DS}) of TPD and spiro-TPD based OTFTs at 290 K. The gate voltage was varied in steps of –10 V starting from 0 to –80 V. Both devices exhibited p-type TFT characteristics with well-defined linear and saturation regions.

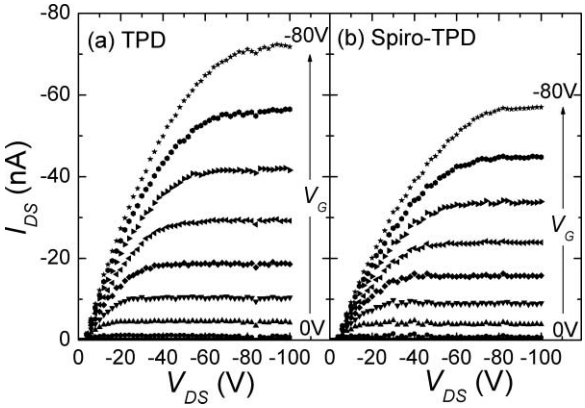

Fig. 3 Output characteristics of top contact (a) TPD and (b) spiro-TPD based OTFTs at 290 K. The gate voltages varied in steps of –10 V between 0 and –80 V.

Plotting $(I_{DS})^{1/2}$ versus V_G, the FE mobility $\mu_{FE,Sat}$ at saturation region (80–100 V) was extracted from slope of the fitting line. $\mu_{FE,Sat}$ of the TPD and spiro-TPD OTFTs were 1.7×10^{-5} and 1.3×10^{-5}cm^2/Vs, respectively,. Correspondingly, we can also extract V_T from the plot of $(I_{DS})^{1/2}$ versus V_G. The threshold voltages are quite small for both TPD (–0.1 V) and spiro-TPD (2.2 V).

Temperature-dependent measurements were carried out for both TPD and spiro-TPD OTFTs between 237 and 359 K. We then analyzed the data by the Gaussian disorder model (GDM).[18] In GDM, each molecule in the amorphous thin film is treated as a transport site for hopping conduction. Under the external field, charge carriers transport within the sites by hopping. The carrier mobility is field- and temperature-dependent and can be described by

$$\mu(F,T) = \mu_\infty \exp[-(2\sigma/3kT)^2] \exp\{CF^{1/2}[(\sigma/kT)^2 - \Sigma^2]\}, \tag{3}$$

where F, T, and k are the applied electric field, the absolute temperature, and the Boltzmann constant, respectively; μ_∞ is the high-temperature limit of mobility, and C is a constant. The energetic disorder σ can be interpreted as the width of Gaussian distribution of the density of states (DOS) of energy for the transporting sites; the positional disorder Σ describes the geometric randomness of the material. At low field ($F\rightarrow0$), the second exponential term in Eq. (3) approaches 1, and thus the temperature-dependence mobility (zero-field mobility μ_0) becomes

$$\mu(0,T) = \mu_0 = \mu_\infty \exp[-(2\sigma/3kT)^2]. \tag{4}$$

The zero-field mobility (μ_0) in each temperature was approximately equal to the FE linear mobility ($\mu_{FE,Lin}$) at low field. $\mu_{FE,Lin}$ can be evaluated from the expression of linear current $I_{DS,Lin}$ [Eq. (1)]. Plotting $I_{DS,Lin}$ versus V_G,$\mu_{FE,Lin}$ at low field ($V_{DS} = -10$ V) was extracted from slope of the fitting line. At room temperature (290 K), the low-field $\mu_{FE,Lin}$ for TPD and spiro-TPD were 9.7×10^{-6} and 7.0×10^{-6}cm^2/Vs, respectively. From Eq. (4), we plotted a graph ln $\mu_{FE,Lin}$ versus $(1/T)^2$. The energetic disorder σ and the high-temperature limit mobility μ_∞ were respectively extracted from the slope and y intercept of the fitted line as shown in Fig. 4. The extracted σ for TPD and spiro-TPD are both ~85 meV. We have compared our results to data from an independent TOF technique.[6,7] Table 1 shows the transport parameters (μ, σ, and μ_∞) of TPD and spiro-TPD in OTFT and TOF techniques.

Two points should be noted from Table 1: (*i*) For both TPD and spiro-TPD, the TFT mobilities extracted in the linear regions are lower than those from the saturation regions. The origin of the discrepancies are most likely related to constact resistances at the *S* and *D* electrodes. For

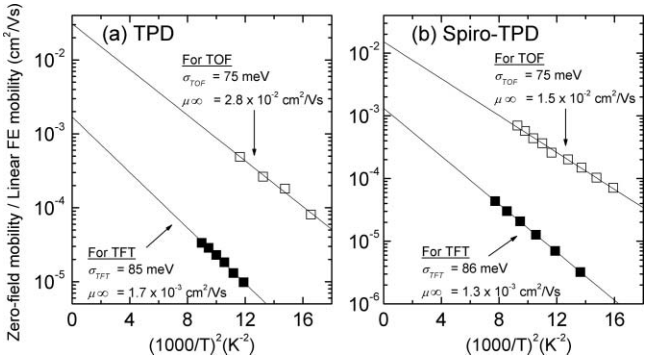

Fig. 4 Field-effect linear mobilities (at $V_{DS} = -10$ V) from TFT and zero-field mobilities ($\tau_{1/2}$) from TOF versus $(1000/T)^2$ for (a) TPD and (b) spiro-TPD. The open and closed symbols are the TOF and TFT data, respectively. The energetic disorders σ and the high-temperature limit mobilities μ_∞ were respectively extracted from the slope and y intercept of the fitted lines.

Table 1 Transport parameters of TPD and spiro-TPD extracted from TFT and TOF.

Material	Technique	Hole mobility at 290 K ($cm^2V^{-1}s^{-1}$)	V_T (V)	σ (meV)	μ_∞ ($cm^2V^{-1}s^{-1}$)
TPD	TFT	1.7×10^{-5} (saturation) 9.7×10^{-6} (linear)	−0.1	85	1.7×10^{-3}
	TOF	4.0×10^{-4}	—	76	2.8×10^{-2}
Spiro-TPD	TFT	1.3×10^{-5} (saturation) 7.0×10^{-6} (linear)	2.2	86	1.3×10^{-3}
	TOF	3.2×10^{-4}	—	75	1.5×10^{-2}

the saturation regions, the contact effects should be negligible as V_{DS} are large (80–100 V). In contrast, contacts between MoO_x and organics only give rise to a voltage drop of a fraction of electron volts. Thus, for the purpose of mobility evaluation, $\mu_{FE,Sat}$ is a more reliable parameter. (*ii*) $\mu_{FE,Sat}$ is one order of magnitude smaller lower than TOF results The reduction in mobility in TFT may arise from scattering of charge carriers by local surface roughness at the gate dielectric. In addition, the increase of the energetic disorder σ [Eq. (3)] is expected to reduce the mobility. According to Borsenberger amd Bässler, the total width of the hopping DOS is the convolution of the intrinsic DOS and extrinsic energetic fluctuations arising from, e.g., polarization in a neighboring medium.[19] If the individual contributions are independent, then the square of total width of the DOS, σ^2_{total} is equal to the sum of the square of the individual contribution. In our experiment, $\sigma^2_{total}$is just σ^2_{TFT}. There are two contributions to σ^2_{TFT}: one is the intrinsic DOS σ^2_{TFT} as obtained from TOF and the additional contribution is due to the random dipoles from the gate dielectric $\sigma^2_{dielectric}$. Combining together these two factors gives rise to

$$\sigma^2_{TFT} = \sigma^2_{TOF} + \sigma^2_{dielectric}. \tag{5}$$

From Eq. (5), the value of $\sigma_{dielectric}$ in both TPD and spiro-TPD was ~40 meV, which is in excellent agreement with other arylamine compounds (NPB and 2TNATA) reported previously.[16] Figure 5 depicts in a schematic diagram why TFT and TOF mobilities should differ.

3.2 *Transport Measurement of Host and Guest Materials in PHOLEDs*

From Sec. 3.1, we establish that it is feasible to use TFT to measure carrier mobilities of amorphous organic materials. Because both TPDs and spiro-TPD contain the same arylamine

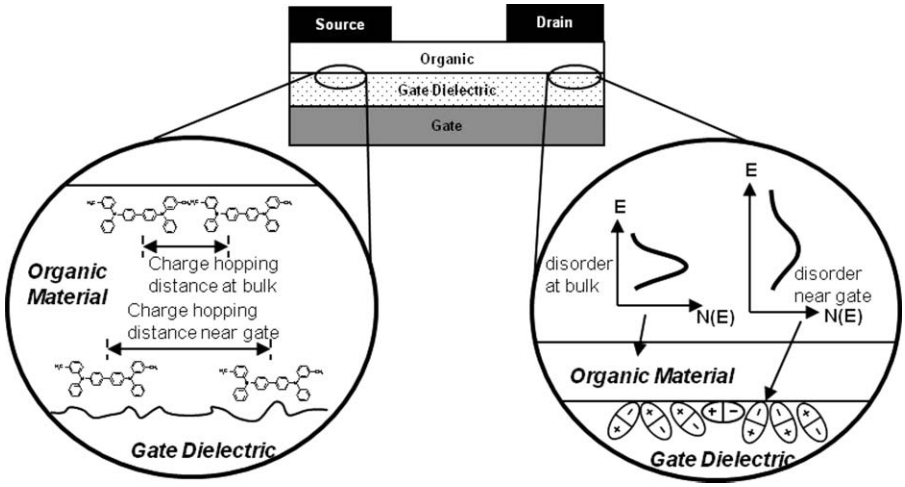

Fig. 5 Schematic diagram showing the surface roughness and polar insulating surface of the gate dielectric. The former effectively increases the charge hopping distance while the latter broadens the energetic disorder.

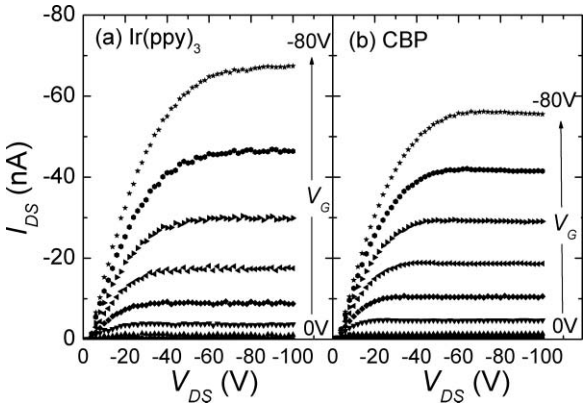

Fig. 6 Output characteristics of top contact (a) $Ir(ppy)_3$- and (b) CBP-based OTFTs at 290 K. The gate voltages varied in steps of −10 V between 0 and –80 V.

functional group, it will be interesting to determine if TFT can be extended to other materials that contain different functional groups. To this end, we extended our study to PHOLED materials $Ir(ppy)_3$ and CBP that contain phenylpyridine and carbazol groups, respectively. Figure 6(a) shows the output characteristics of a pristine $Ir(ppy)_3$ film at room temperature (292 K). The current–voltage curves show well-defined *p*-type characteristics. From Eqs. (1) and (2), the hole mobility of $Ir(ppy)_3$ can be extracted.[20] The results are $\mu_{\text{Lin}} = 9.5\times10^{-6}$ $\text{cm}^2\text{V}^{-1}\text{s}^{-1}$ and $\mu_{\text{Sat}} = 1.7\times10^{-5}$ $\text{cm}^2\text{V}^{-1}\text{s}^{-1}$. The mobility values are in the range of a typical amorphous organic hole transporter in OLED applications. For example, NPB, is a commonly used hole-transporting material for OLEDs. The FE mobility is 2.4×10^{-5} $\text{cm}^2\text{V}^{-1}\text{s}^{-1}$ as measured by the TFT technique in the saturation region.[21] Judging from the hole mobility values, $Ir(ppy)_3$ can be viewed as a good hole transporter.

Figure 6(b) shows the output characteristics of a pristine CBP film at room temperature (292 K). In spite of a relative large HOMO level (∼5.8 eV) of CBP, well-behaved output characteristics can still be observed. The result indicates that MoO_x can indeed possess a high work function to facilitate hole injections into CBP. This finding is actually consistent with a previous publication.[22] Applying the same approach as $Ir(ppy)_3$, the hole mobilities of CBP are $\mu_{\text{Lin}} = 1.2\times10^{-5}$ $\text{cm}^2\text{V}^{-1}\text{s}^{-1}$ and $\mu_{\text{Sat}} = 1.5\times10^{-5}$ $\text{cm}^2\text{V}^{-1}\text{s}^{-1}$ in the linear and saturation, respectively.

We have established that $Ir(ppy)_3$ is actually a good hole transporter. Its transport mechanism was further investigated by temperature-dependent measurements. The results were analyzed by the GDM, which is outlined in Sec. 3.1. Figure 7 shows the semi-log plots of linear FE mobilities

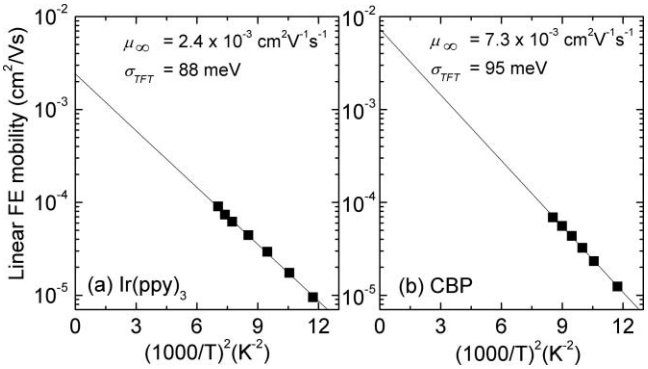

Fig. 7 FE linear mobilities (at $V_{\text{DS}} = -10$ V) from TFT versus $(1000/T)^2$ for (a) $Ir(ppy)_3$ and (b) CBP. The energetic disorders σ and high-temperature limit mobilities μ_∞ were respectively extracted from the slope and *y* intercept of the fitted lines.

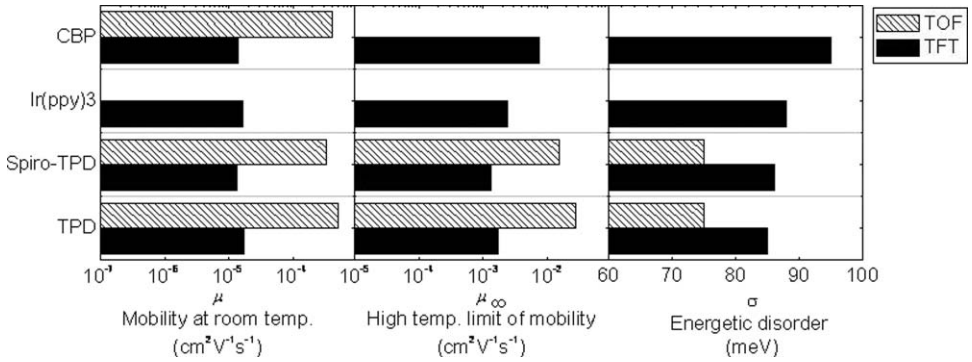

Fig. 8 Transport parameters of TPD, spiro-TPD, Ir(ppy)3, and CBP extracted from TFT and TOF (CBP's TOF data from literature; see Refs. 24 and 25).

versus $(1000/T)^2$ of $Ir(ppy)_3$ and CBP OTFTs, respectively. The extracted σ for $Ir(ppy)_3$ in an OTFT is 88 meV. It is comparable to the data from other amorphous organic hole transporters measured by the TFT technique, such as phenylamine compounds (e.g., NPB).[15,16,23] In those cases, the range of σ is within 80–90 meV. The extracted σ and μ_∞ of pristine CBP are 95 meV and 7.3×10^{-3} $cm^2V^{-1}s^{-1}$, respectively. Figure 8 is a summary of the transport parameters of the four materials in this work.

$Ir(ppy)_3$ is often a dopant in CBP rather than a host.[26–28] Therefore, it is more meaningful to study the hole transport properties in a $Ir(ppy)_3$-doped CBP film. The inset in Fig. 9 shows the TFT output characteristics of a 20% $Ir(ppy)_3$-doped CBP film. The output current I_{DS} is dramatically decreased compared to a 100% $Ir(ppy)_3$ film. The FE mobility is $\mu_{Sat} = 1.7 \times10^{-7}$ $cm^2V^{-1}s^{-1}$, evaluated in the saturation region. The value is two orders of magnitude smaller than the pristine $Ir(ppy)_3$ film. Figure 9 shows the hole mobility μ_{Sat} of $Ir(ppy)_3$-doped CBP films at different doping concentrations. In the system of $Ir(ppy)_3$-doped CBP, we realize a large HOMO difference between CBP and $Ir(ppy)_3$ (~0.5 eV). Thus, $Ir(ppy)_3$ molecules can be regarded as deep traps. In principle, holes can be injected from the source electrode, through the MoO_x interlayer, into both CBP and $Ir(ppy)_3$ molecules. Injection of holes into $Ir(ppy)_3$, however, is energetically more favorable. At a low doping level (e.g., <10%), once holes are injected, hopping among the dopant molecules is not preferable due to a longer hopping distance. Injected holes can only hop among the host molecules but may be trapped by dopant

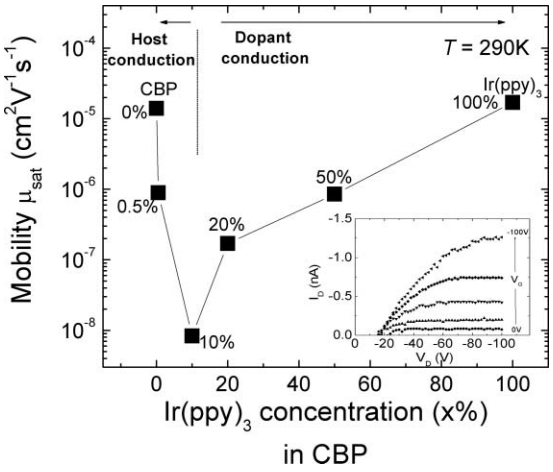

Fig. 9 Saturation mobility μ_{Sat} of CBP:$Ir(ppy)_3$ OTFT film versus doping concentration. Inset: TFT output characteristics of a 20% $Ir(ppy)_3$-doped CBP film.

molecules. Thus, it is expected that hole mobility decreases with the doping concentration. In contrast, at a sufficient high doping concentration (e.g., >10%), holes are likely to hop among the dopant molecules rather than the host because of reduced hopping distances. Thus, it is expected that hole mobility reaches at a optimized value and gradually increases with the doping concentration. Actually, at 10% of doping concentration, the TFT signals were barely detectable at room temperature (290 K) and the mobility value was evaluated from a higher temperature (394 K).

4 Conclusion

In this contribution, we employ TFT technique to study carrier transport in amorphous organic electronic materials. Compared to other techniques (e.g., TOF, dark-injection space-charge-limited current, and *JV* characteristic), TFT only consumes small quantities of materials. Although we used a film thickness of 100 nm in our experiments, the film thickness, in principle, can be reduced to <10 nm because only several monolayers of molecules are needed to form a complete conducting channel. We studied hole transport in the spiro-TPD- and TPD-based TFTs. The data are comparable to an independent TOF technique. Thus, TFT can be viewed as a powerful platform for mobility determination when the material under investigation is in limited quantity. Besides arylamine compounds, we have extended our studies to the phosphorescent organic light emitter $Ir(ppy)_3$, host material CBP, and $Ir(ppy)_3$-doped CBP.

Acknowledgments

Support of this research by the Research Committee of Hong Kong Baptist University and the Research Grant Council of Hong Kong under Grant No. FRG2/09–10/077 and HKBU211209E are gratefully acknowledged.

References

1. C. W. Tang and S. A. VanSlyke, "Organic electroluminescent diodes," *Appl. Phys. Lett.* **51**, 913–915 (1987).
2. G. Horowitz, "Organic thin film transistors: From theory to real devices," *J. Mater. Res.* **19**, 1946–1962 (2004).
3. P. Peumans, A. Yakimov, and S. R. Forrest, "Small molecular weight organic thin-film photodetectors and solar cells," *J. Appl. Phys.* **93**, 3693–3723 (2003).
4. S. Reineke, F. Lindner, G. Schwartz, N. Seidler, K. Walzer, B. Lüssem, and K. Leo, "White organic light-emitting diodes with fluorescent tube efficiency," *Nature* **459**, 234–238 (2009).
5. S. K. So, S. C. Tse, and C. H. Cheung, *Organic Electronics: Materials, Processing, Devices and Applications*, F. So, Ed., Chap. 3, CRC Press, Taylor and Francis, Boca Raton, FL (2010).
6. S. K. So, S. C. Tse, and K. L. Tong, "Charge transport and injection to phenylamine-based hole transporters for OLEDs applications," *J. Disp. Technol.* **3**, 225–232 (2007).
7. W. H. Choi and S. K. So, "Charge injection and transport in spiro-linked arylamine compounds," *Proc. SPIE* **7415**, 74151L (2009).
8. D. Yokoyama, A. Sakaguchi, M. Suzuki, and C. Adachi, "Horizontal molecular orientation in vacuum-deposited organic amorphous films of hole and electron transport materials," *Appl. Phys. Lett.* **93**, 173302 (2008).
9. D. Yokoyama, A. Sakaguchi, M. Suzuki, and C. Adachi, "Horizontal orientation of linear-shaped organic molecules having bulky substituents in neat and doped vacuum-deposited amorphous films," *Org. Electron.* **10**, 127–137 (2009).
10. M. E. Kondakova, T. D. Pawlik, R. H. Young, D. J. Giesen, D. Y. Kondakov, C. T. Brown, J. C. Deaton, J. R. Lenhard, and K. P. Klubek, "High-efficiency, low-voltage

phosphorescent organic light-emitting diode devices with mixed host," *J. Appl. Phys.* **104**, 094501 (2008).
11. M. H. Ho, B. Balaganesan, T. Y. Chu, T. M. Chen, and C. H. Chen, "A morphologically stable host material for efficient phosphorescent green and red organic light emitting devices," *Thin Solid Films* **517**, 943–947 (2008).
12. C. H. Cheung, W. J. Song, and S. K. So, "Role of air exposure in the improvement of injection efficiency of transition metal oxide/organic contact," *Org. Electron.* **11**, 89–94 (2010).
13. K. Kanai, K. Koizumi, S. Ouchi, Y. Tsukamoto, K. Sakanoue, Y. Ouchi, and K. Seki, "Electronic structure of anode interface with molybdenum oxide buffer layer," *Org. Electron.* **11**, 188–194 (2010).
14. W. Song, S. K. So, and L. Cao, "Angular-dependent photoemission studies of indium tin oxide surface," *Appl. Phys. A* **72**, 361–365 (2001); M. Kröger, S. Hamwi, J. Meyer, T. Riedl, W. Kowalsky, and A. Kahn, "Role of the deep-lying electronic states of MoO_3 in the enhancement of hole-injection in organic thin films," *Appl. Phys. Lett.* **95**, 123301 (2009).
15. C. H. Cheung, K. K. Tsung, K. C. Kwok, and S. K. So, "Using thin film transistors to quantify carrier transport properties of amorphous organic semiconductors," *Appl. Phys. Lett.* **93**, 083307 (2008).
16. C. H. Cheung, K. C. Kwok, S. C. Tse, and S. K. So, "Determination of carrier mobility in phenylamine by time-of-flight, dark-injection, and thin film transistor techniques," *J. Appl. Phys.* **103**, 093705 (2008).
17. S. M. Sze, *Physics of Semiconductor Devices*, Wiley, Hoboken, NJ (1981).
18. H. Bässler, "Charge transport in disordered organic photoconductors - a monte-carlo simulation study," *Phys. Stat. Soidi. B* **175**, 15–56 (1993).
19. P. M. Borsenberger and H. Bässler, "Concerning the role of dipolar disorder on charge transport in molecularly doped polymers," *J. Chem. Phys.* **95**, 5327–5331 (1991).
20. W. H. Choi, C. H. Cheung, and S. K. So, "Can an organic phosphorescent dye act as a charge transporter?," *Org. Electron.* **11**, 872–875 (2010).
21. S. C. Tse, K. C. Kwok, and S. K. So, "Electron transport in naphthylamine-based organic compounds," *Appl. Phys. Lett.* **89**, 262102 (2006).
22. M. Kröger, S. Hamwi, J. Meyer, T. Riedl, W. Kowalsky, and A. Kahn, "P-type doping of organic wide band gap materials by transition metal oxides: A case-study on Molybdenum trioxide," *Org. Electron.* **10**, 932–938 (2009).
23. T. P. I. Saragi, T. F. Lieker, and J. Salbeck, "Comparison of charge-carrier transport in thin films of spiro-linked compounds and their corresponding parent compounds," *Adv. Funct. Mater.* **16**, 966–974 (2006).
24. N. Matsusue, Y. Suzuki, and H. Naito, "Charge carrier transport in neat thin films of phosphorescent iridium complexes," *Jpn. J. Appl. Phys.* **44**, 3691–3694 (2005).
25. S. B. Lee, T. Yasuda, M. J. Yang, K. Fujita, and T. Tsutsui, "Charge carrier mobility in vacuum-sublimed dye films for light-emitting diodes studied by the time-of-flight technique," *Mol. Cryst. Liq. Cryst.* **405**, 67–73 (2003).
26. M. A. Baldo, D. F. O'Brien, Y. You, A. Shoustikov, S. Sibley, M. E. Thompson, and S. R. Forrest, "Highly efficient phosphorescent emission from organic electroluminescent devices," *Nature* **395**, 151–154 (1998).
27. M. A. Baldo, S. Lamansky, P. E. Burrows, M. E. Thompson, and S. R. Forrest, "Very high-efficiency green organic light-emitting devices based on electrophosphorescence," *Appl. Phys. Lett.* **75**, 4–6 (1999).
28. T. Sajoto, P. Djurovich, A. B. Tamayo, J. Oxgaard, W. A. Goddard III, and M. E. Thompson, "Temperature dependence of blue phosphorescent cyclometalated Ir(III) complexes," *J. Am. Chem. Soc.* **131**, 9813–9822 (2009).

Biographies and photographs of the authors not available.